Nitrone/Imine Selectivity Switch in Base-Catalysed Reaction of Aryl Acetic Acid Esters with Nitrosoarenes: Joint Experimental and Computational Study

DOI: 10.1002/adsc.202((will be filled in by the editorial staff))

Nitrone/Imine Selectivity Switch in Base-Catalysed Reaction of Aryl Acetic Acid Esters with Nitrosoarenes: Joint Experimental and Computational Study

Chiara Volpe,[a] Sara Meninno,[a] Angelo Roselli,[a] Michele Mancinelli,[b] Andrea Mazzanti*[b] and Alessandra Lattanzi*[a]

[a] Dipartimento di Chimica e Biologia "A. Zambelli", Università di Salerno
Via Giovanni Paolo II, 132, 84084 Fisciano, Italy
E-mail: lattanzi@unisa.it

[b] Department of Industral Chemistry "Toso Montanari", University of Bologna
Viale Risorgimento 4, 40146 Bologna, Italy
E-mail: andrea.mazzanti@unibo.it

Received: ((will be filled in by the editorial staff))

Supporting information for this article is available on the WWW under http://dx.doi.org/10.1002/adsc.201######.((Please delete if not appropriate))

Abstract. Herein we report a mild and diastereoselective access to ketonitrones by reacting easily available aryl acetic acid esters and other active methylene compounds, with nitrosoarenes under catalytic loading of 2-*tert*-butylimino-2-diethylamino-1,3-dimethylperhydro-1,3,2-diazaphosphorine (BEMP) at room temperature. Depending on the substitution pattern and nature of the aryl moiety, a switch toward the formation of imines can be observed. The mechanistic framework is put to scrutiny by experimental and theoretical studies, pointing to the formation of a nitroso aldol intermediate, whose fate toward one of the competing pathways, namely hydride transfer or elimination, would depend upon the NOH/CH$_\alpha$ relative acidities.

Keywords: nitrones; catalysis; imines; nitrosoarenes; BEMP

Introduction

Nitrones are 1,3-dipoles, frequently used as the reagents of choice for the synthesis of a great array of heterocyclic compounds, likely being isoxazolines and isoxazolidines the most popular.[1] Taking advantage of [3+2]-, [3+3]-, [4+2]-, [4+3]-dipolar cycloaddition reactions, three- to seven- membered nitrogen and oxygen containing heterocycles are built with high atom-economy.[2] The configurational stability of nitrones and chelation or H-bonding acceptor abilities of the oxygen atom, make them versatile reagents for the development of stereocontrolled variants.[3] The asymmetric Kinugasa reaction between terminal alkynes and nitrones, exemplifies a facile entry to β-lactams, which are scaffolds of notable interest in the pharmaceutical industry.[4] Nitrones are of synthetic utility in other important transformations such as aldol-type,[5] Friedel-Crafts,[6] electrocyclization,[7] rearrangement reactions.[8]

Unsurprisingly, different procedures for their preparation have been developed over the years, such as the condensation of *N*-monosustituted hydroxyl amine with aldehydes and ketones (Scheme 1 A(i)),[9] the oxidation of secondary amines, hydroxyl amines and imines (Scheme 1A(ii)),[10] reaction of oximes with electrophiles or alkenes often useful to access cyclic nitrones (Scheme 1 A(iii)).[11] The most common and effective method to prepare nitrones is the condensation of hydroxyl amines (Scheme 1 A(i) with aldehydes as the reagent. However, this approach appears less useful when targeting ketonitrones, which are in general more difficult to access.

A less explored approach to nitrones involves the use of nitrosoarenes as the reagents, a class of versatile and readily available electrophiles.[12] They proved to be useful in the Au/Ag-catalysed 1,2-iminonitronation of propargylic esters to give α-imidoyl nitrones (Scheme 1 B(i),[13] or in the organocatalytic addition of the γ-nitrone group onto the α,β-unsaturated aldehydes (Scheme 1 B(ii)).[14] Interestingly, an umpolung strategy (Scheme 1 B(iii)), alternative to route A(i), has been devised using α-keto methyl esters under stoichiometric amounts of phosphines to produce ketonitrones.[15] The latter are versatile building blocks to prepare imines, fumarates and isoxazolines. A direct approach using nitrosoarenes has been demonstrated on specific carbanions, bearing leaving groups.[16]

We recently developed a variant of the Ehrlich-Sachs reaction, reported in 1899 as the condensation

between active methylene compounds and nitroso derivatives.[17] This process, whose mechanism is still unclear, usually proceeds under basic catalysis, giving imines or nitrones in a ratio that is difficult to predict. Our methodology provided an effective α-imination of acyl pyrazoles, working under mild conditions and using a catalytic amount of a base (Scheme 1C).[18]

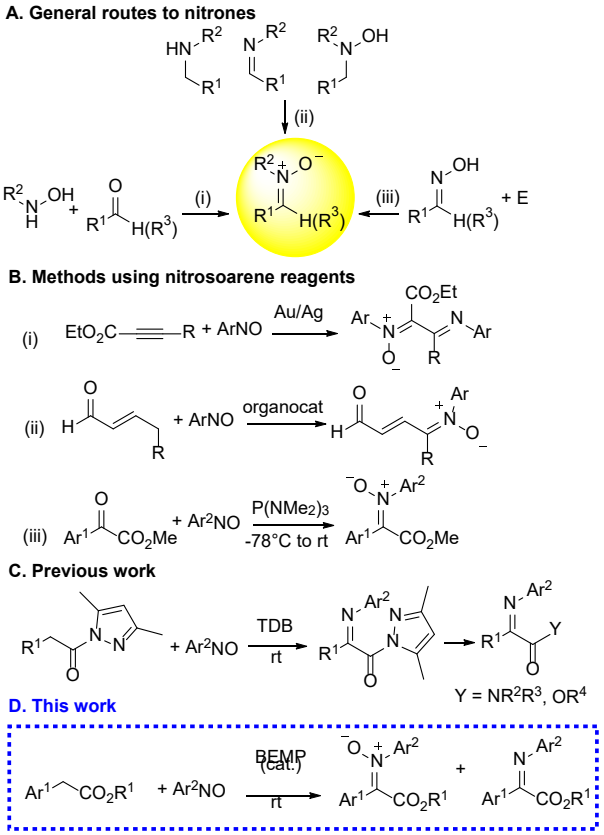

Scheme 1. General and nitrosoarene based routes to nitrones.

High chemical selectivity was observed, although traces of nitrones were occasionally detected, when using compounds less prone to enolate formation. Intrigued by this observation, we questioned whether a similar approach could be applied to access ketonitrones, by reacting easily available aryl acetic acid esters, which are notoriously less acidic at the α-position than the corresponding acyl pyrazoles (Scheme 1D).[19] This would open a direct and convenient route to ketonitrones, alternative to route B(iii) (Scheme 1). Moreover, we investigated the issues affecting the nitrone/imine selectivity and the overall mechanistic framework, by means of experimental and computational studies, to pursuit a better understanding of the Ehrlich-Sachs type reaction, useful for further applications.

Results and Discussion

In order to assess our hypothesis, we started the study by reacting commercially available phenyl acetic acid methyl ester with nitrosobenzene, under previously optimized reaction conditions,[18] in the presence of 10 mol% 1,5,7-triazabicyclo[4.4.0]dec-5-ene (TBD) and 3Å molecular sieves, at room temperature in CH_2Cl_2 (Table 1, entry 1).

Table 1. Optimization study on the reaction of **1a** with PhNO under basic catalysis. [a]

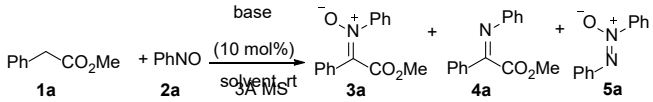

Entry	Base	Solvent	t (h)	Yield **3a** (%)[b]	Yield[b] **4a** (%) [**5a**] (%)]
1[c]	TBD	CH_2Cl_2	1	30 (93/7)	- [27]
2	TBD	CH_2Cl_2	1	79 (93/7)	2 [82]
3	TBD	toluene	2.5	70 (93/7)	14 [74]
4	TBD	THF	1	51(92/8)	15 [56]
5	TBD	$CHCl_3$	1	47 (93/7)	- [49]
6	TBD	$Cl(CH_2)_2Cl$	1	49 (93/7)	5 [53]
7	TBD	AcOEt	3	62 (94/6)	27 [57]
8[d]	TBD	CH_2Cl_2	1	73 (93/7)	4 [nd]
9	DBU	CH_2Cl_2	3	61 (92/8)	- [60]
10	TMG	CH_2Cl_2	1	-	-
11	Et_3N	CH_2Cl_2	1	-	-
12	BEMP	CH_2Cl_2	1	87 (95/5)	3 [84]
13[e]	BEMP	CH_2Cl_2	1	35 (95/5)	4 [36]

[a] Reaction conditions: 0.2 mmol of **1a**, 0.6 mmol of **2a**, 0.02 mmol of base, 50 mg of 3 Å MS in anhydrous solvent (1 mL). [b] Isolated yields after column chromatography. In parenthesis *E*/*Z* ratio. [c] 1.2 eq. of **2a** were used. [d] 3.5 eq. of **2a** were used. [e] BEMP was used at 5 mol % loading.

Pleasingly, the selective formation of nitrone **3a** was observed in 30% yield and 93/7 *E*/*Z* ratio without observing traces of imine **4a**. In order to improve the conversion to **3a,** three equivalents of **2a** were added (entry 2). After the same time, nitrone **3a** was selectively isolated in 79% yield. A brief solvent screening showed that the amount of imine, although low, was affected by the nature of the solvent (entries 3, 4 and 7). The conversion to nitrone did not benefit of increased amount of **2a** (entry 8). Next, different bases were checked under the conditions reported in entry 2. 1,5-Diazabiciclo(5.4.0)undec-7-ene (DBU) proved to be selective, but less efficient than TBD (entry 9). Less basic 1,1,3,3-tetramethylguanidine (TMG) and Et_3N did not promote the reaction (entries 10 and 11). Conversely, when a stronger base like 2-*tert*-butylimino-2-diethylamino-1,3-dimethylperhydro -1,3,2-diazaphosphorine (BEMP) was used, **3a** was selectively obtained in 87% yield and 95/5 *E*/*Z* ratio (entry 12). However, a decrease of BEMP loading to 5 mol% negatively affected the conversion to **3a** (entry 13).

Having established the best reaction conditions (Table 1, entry 12) the scope and limitations of the reaction was investigated (Table 2). Pleasingly, phenyl acetic acid methyl esters bearing halogen atoms at different positions and the *meta*-methoxy

derivative were rapidly transformed into the corresponding ketonitrones **3b-g** in high yield and diastereoselectivity, observing imines in traces.

Table 2. Substrate scope of BEMP-catalysed reaction of aryl acetic acid esters **1** with nitrosobenzene **2a**.[a]

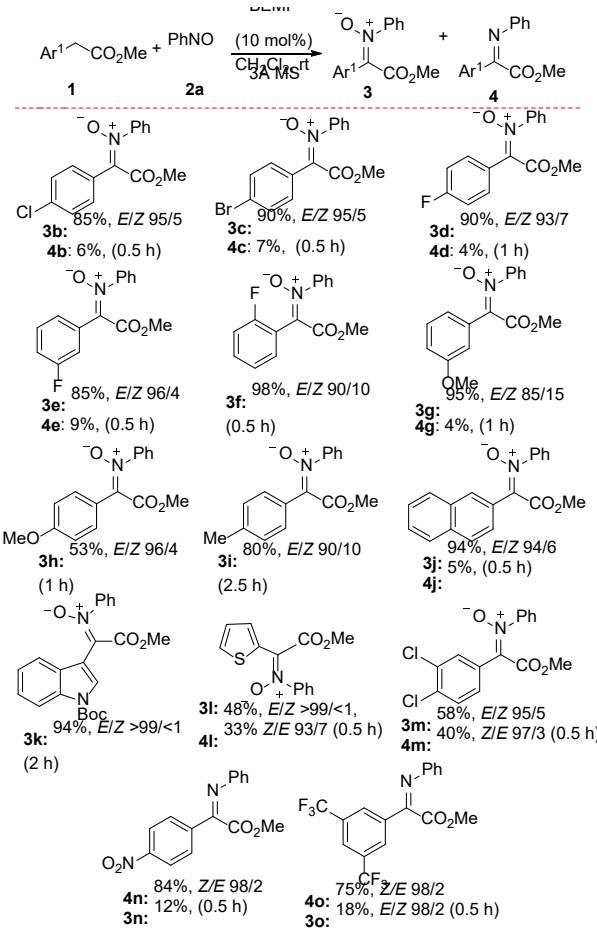

[a] Reaction conditions: 0.4 mmol of **1**, 1.2 mmol of **2a**, BEMP (0.04 mmol), 3 Å MS in CH_2Cl_2 (2 mL). Isolated yields after column chromatography.

Phenyl acetic acid methyl esters, bearing electron-donating groups at *para*-position, were exclusively converted into ketonitrones **3h**,**i** in good yield and high *E*/*Z* ratio. 2-Naphthyl and the *N*-Boc-3-indolyl acetic acid methyl esters afforded nitrones **3j**,**k** in excellent yield and diastereoselectivity. When reacting compounds **1l**,**m** both nitrones **3l**,**m** and imines **4l**,**m** were formed in comparable yields. Substrates bearing electron-withdrawing groups afforded imines **4n**,**o** in high *Z*/*E* ratio and low amounts of nitrones **3n**,**o** were detected. The applicability of the process was further assessed using other aryl acetic acid esters and nitrosoarenes under the same reaction conditions (Table 3). Differently substituted nitrosoarenes were well tolerated when reacted with a variety of aryl acetates bearing linear or sterically more demanding R^1 groups, leading to nitrones **3p,s** in good yields and high diastereoselectivity. When a strong electron-withdrawing group was present in the phenyl group of the ester, the exclusive formation of the *Z*-imine **4t** in excellent yield was observed.

Table 3. Scope of esters and aryl nitroso compounds in the BEMP-catalysed reaction.[a]

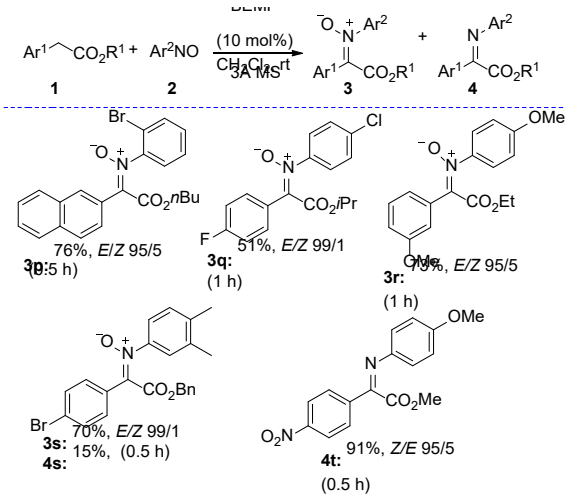

[a] Reaction conditions: 0.4 mmol of **1**, 1.2 mmol of **2**, BEMP (0.04 mmol), 3 Å MS in CH_2Cl_2 (2 mL). Isolated yields after column chromatography.

The efficiency of the system to selectively yield imines when using easily enolizable carbonyls such as 1,3-dicarbonyl compounds, pyrazolones and indolinones with nitrosobenzene **2a** was therefore studied (Table 4).

Table 4. BEMP-catalysed α-imination of more acidic carbonyl compounds with nitrosobenzene.[a]

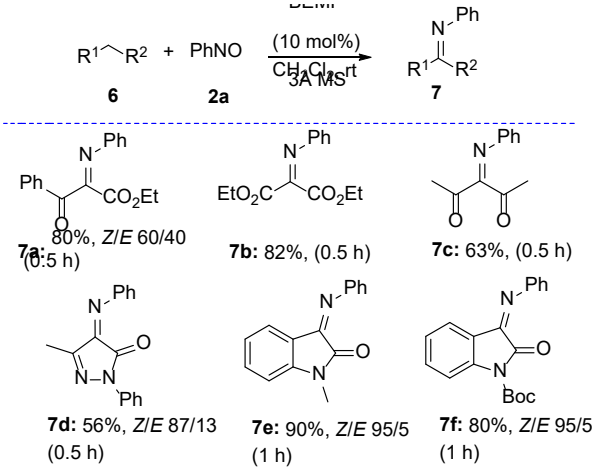

[a] Reaction conditions: 0.4 mmol of **1**, 1.2 mmol of **2**, BEMP (0.04 mmol), 3 Å MS in CH_2Cl_2 (2 mL). Isolated yields after column chromatography.

As expected, commercially available β-ketoesters, malonate and β-diketones, as well as pyrazolone and *N*-protected indolinones, were rapidly transformed into the corresponding imines **7a-c** in fairly good yields, observing moderate to high *E*/Z ratios.

Finally, we demonstrated that ketonitrones **3** can be of further synthetic utility to prepare 2,3,4-triaryl-substituted 1,2,4-oxadiazole-5-ones. In this regard,

Campisi and coworkers recently demonstrated that 2,3,4-triaryl-substituted 1,2,4-oxadiazole-5-ones showed significant cytotoxic effect in the MCF-7 human breast cancer cell line,[20] behaving as cyclic analogues of tamoxifen. Novel 2,3,4-triaryl-substituted-3-carbalcoxy-1,2,4-oxadiazole-5-ones bearing a quaternary stereocenter, were regioselectively obtained in high yield via 1,3-dipolar cycloaddition of representative ketonitrones **3a,k** with arylisocyanates **8** (Scheme 2).

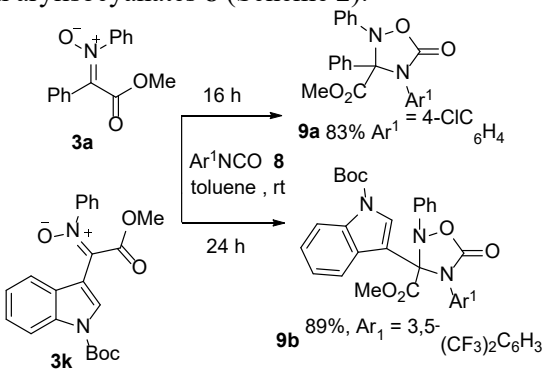

Scheme 2. 1,3-Dipolar cycloaddition of ketonitrones with arylisocianates.

In order to shed light on the mechanism of the reaction some experiments were carried out. A model reaction between compound **1a** (Table 1, entry 12) and **2a** was performed in the presence of the radical scavenger TEMPO (1.1 eq.) (Scheme 3).

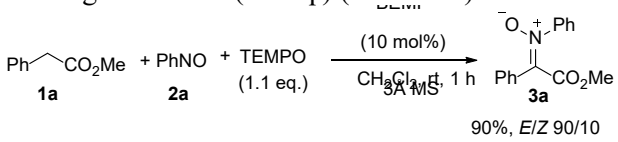

Scheme 3. Model reaction in the presence of radical scavenger TEMPO.

The reaction appeared unaffected by the presence of the radical scavenger, as shown by the recovered nitrone **3a** in 90% yield and 90/10 E/Z ratio. Moreover, model reaction (Table 1, entry 12) was monitored in CD_2Cl_2 via ^{1}H-NMR over time, to check if radical species would be involved. Both the experiments confirmed the absence of any detectable radical species or other potential intermediates, such as nitrosoaldol species. Hence, all the data suggest that radical pathways are not involved during the reaction. According to experimental data, literature precedents and our own report,[18] we suggest a mechanistic proposal for the reaction of aryl acetic acid esters and nitrosobenzene catalyzed by BEMP (Figure 1).

In the first reaction stage, BEMP removes the α-hydrogen of the ester to generate the enolate, that subsequently adds to nitrosobenzene to yield intermediate **I** (10 mol%).

At this stage the reaction forks into two different pathways. When tautomerism takes place by the action of a base to yield the nitrosoenolate, an $E1_{CB}$ elimination drives the reaction towards the imine **4**. In the other side, the excess nitrosobenzene can oxidize the nitrosoaldol to nitrone **3** with the formation of azoxybenzene **5**. Both branches of the catalytic cycle yield an equivalent of OH^- that sustains the catalytic cycle by deprotonating the starting ester. Within the whole catalytic cycle, the roles of BEMP and $BEMPH^+$ are to trigger the first formation of ester enolate, to coordinate the anionic species within the catalytic cycle, and to act as hydrogen bonding donor when feasible.

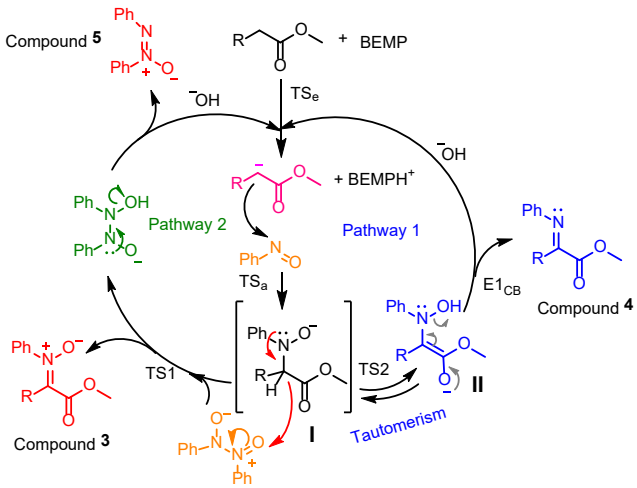

Figure 1. Proposed catalytic cycle for the nitrone/imine formation.

The proposed reaction scheme implies the formation of comparable amount of **5** and nitrone **3**. This correspondence was experimentally observed in all the cases where the nitrone yield was not negligible (see Table 1).

The ability of nitrosobenzene to oxidize *via* hydride transfer has been previously documented either under acidic or basic conditions.[21] To check the feasibility of hydride transfer under our reaction conditions, diphenyl carbinol **10** was treated with PhNO (2 eq.) and BEMP (1 eq.) in CH_2Cl_2 at room temperature under nitrogen (Scheme 4).

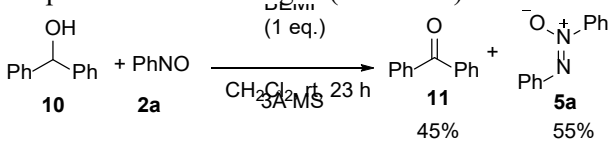

Scheme 4. Oxidation of diphenyl carbinol by BEMP/PhNO system.

Interestingly, the formation of benzophenone **11** was observed in 45% yield. This experiment would support the occurrence of hydride migration by intermediate **I** to nitrosobenzene, which behaves as popular hydride acceptors such as DDQ and DQ.[22]

Finally, we demonstrated that the reaction pathway can be diverted according to the reaction conditions,

using ester **1c** which afforded nitrone **3c** (Table 2) in high yield under usual conditions (Scheme 5).

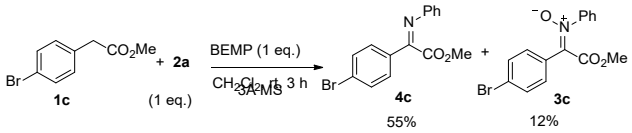

Scheme 5. Reversal of reaction pathway toward imine product.

A slow addition of BEMP (1 eq.) to ester **1c** was followed by a one hour addition of a solution of **2a** at room temperature. Under these conditions, we expected to push the reaction towards the imine pathway, given the very low concentration of free nitrosobenzene present in the reaction mixture, combined with a significant presence of the ester enolate. Indeed, imine **4c** was isolated as the prevalent product in 55% yield and only 12% of nitrone **3c** was recovered.

The effectiveness of BEMP and OH^- (as $BEMPH^+OH^-$) in the formation of the enolate of model ester **1a** was checked via ^{1}H-NMR analysis in CD_2Cl_2. The reaction mixture of **1a** and BEMP (1 eq.) was quenched after 30 minutes by adding excess D_2O and the determination of α-monodeuterated and α,α-dideuterated ester was evaluated over 1 hour time. It was found that deuteration at the α positions did not stop after the D_2O quenching.[23]

Theoretical study

A theoretical study of the catalytic cycle was performed using DFT calculations and using **1a** as the model compound and B3LYP/6-31G(d). When localized, the stationary points were further optimized using the M06-2X/6-311+G(d,p) level.

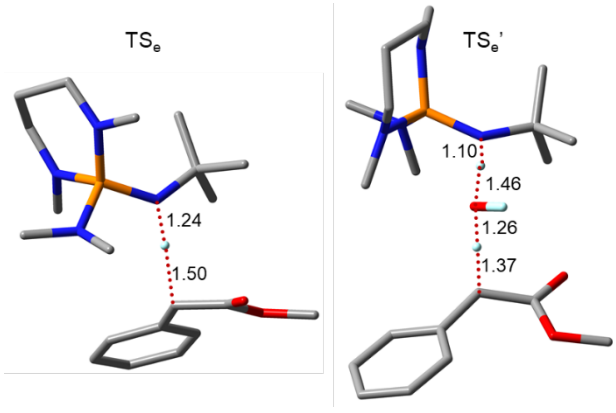

Figure 2. TS_e geometry for enolization of **1a** by BEMP (left) and by $BEMPH^+OH^-$ (TS_e'). Only the relevant hydrogens are shown. Distances in Å.

In the first reaction stage, BEMP removes one H_α from the ester to yield the enolate.[25] In the optimized TS_e structure the C-H distance was 1.50 Å, while the N-H distance was 1.24 Å.[26] With respect to the reagents, TS_e had an activation energy of 19.0 kcal/mol. However, this TS is valid only at the beginning of the reaction, when neutral BEMP is present. For the sustainment of the catalytic cycle, enolization of the starting reagent has to be carried on also by the hydroxyl anion that is generated by both the branches of the proposed catalytic cycle (Figure 1, left). Being dichloromethane the reaction solvent, the presence of free and unsolvated OH^- is not realistic, so we considered that the active base for enolization is the ionic pair $BEMPH^+OH^-$. A second TS geometry was built with these requisites and optimized (TS_e', right in Figure 2), with a calculated energy of 27.8 kcal/mol.

Once the enolate is formed, the addition reaction with nitrosobenzene yields intermediate **I**. For this step it should be considered that the $BEMPH^+$ cation coordinates the enolate at the anionic oxygen in the reagent, while it shifts on the negative oxygen of the $ArNO^-$ at the end of the reaction.

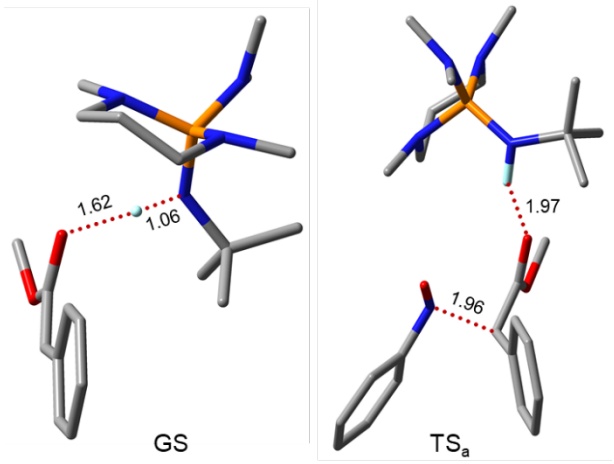

Figure 3. Left: GS geometry of the enolate complex of **1a** with $BEMPH^+$. Right: TS_a geometry for addition of the same enolate to PhNO. Only the relevant hydrogens are shown. Distances in Å.

The optimized TS_a geometry illustrated in Figure 3 shows that $BEMPH^+$ is between the two oxygens and it moves from the enolic oxygen to the oxygen of PhNO while the C-N bond is formed. The C-N distance in the TS_a geometry was 1.96 Å, and the activation energy was found to be 28.5 kcal/mol. At the end of the addition step, the nitrosoaldolate **I** is formed, with a relative energy with respect to the reagents as low as -9.6 kcal/mol (Figure 4). Since no intermediates were observed in the NMR monitoring of the reaction, the kinetically relevant TS for the whole reaction has to be found either in the first enolization step with $BEMPH^+OH^-$ or in the subsequent addition to PhNO.

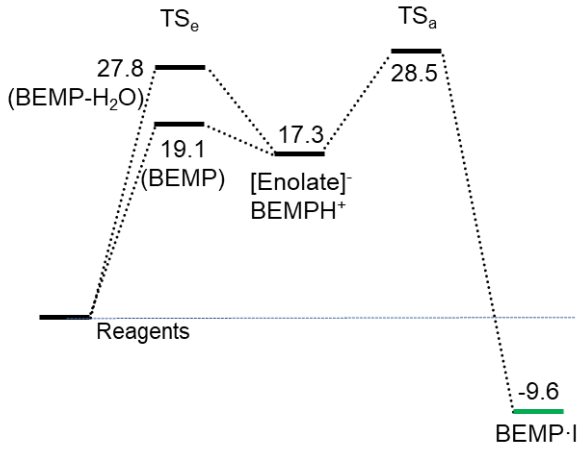

Figure 4. First section of the catalytic pathway for compound **1a**. Energies in kcal/mol at the M06-2X/6-311+G(d,p) level.

The feasibility of the enolate addition to the dimer of nitrosobenzene[27] was evaluated via the calculation of the electrofilicity index ω as proposed by Parr.[28] It was found that the monomer had ω = 1.99 eV, whereas the dimer had ω = 1.55 eV (M06-2X/6-311+G(d,p) level). Thus, the nucleophilic attack of the enolate onto the nitrosobenzene monomer is strongly favored.

After the addition to nitrosobenzene, intermediate **I** can exist as an ionic pair of the nitrosoaldolate with BEMPH$^+$, or as a nitrosoaldol/BEMP complex. Calculations suggested that the latter situation is more stable by 5.2 kcal/mol, and that the TS involved in the hydrogen shift from the nitrogen of BEMP to the oxygen of the nitrosoaldolate is very small (3.0 kcal/mol starting from the ionic pair, see Figure S1 in Supporting Information). Thus, the two forms can easily exchange into each other. DFT optimization of intermediate **I** with three selected substituents (4-$NO_2C_6H_4$ **In**, 4-$MeOC_6H_4$ **Ih** and 3,4-$Cl_2C_6H_3$ **Im**) showed very similar energy profiles for the formation of intermediate **I** (see Figure S2 of the Supporting Information).

Oxidative pathway to nitrone 3

Nitrone **3a** can be obtained via oxidation of the nitrosoaldolate by the PhNO or $(PhNO)_2$ still present in the reaction mixture. First, the hydrogen shift to form the nitrosoaldolate/BEMPH$^+$ ionic pair is required, followed by the hydride abstraction step to yield nitrone **3a**.[29] In the transition state for the reaction with PhNO (Figure S3 in the Supporting Information)[21] the C-H and H-O distances were 1.50 Å and 1.13 Å, respectively.[30] The resulting phenyl hydroxylamine anion then adds to PhNO still present in the reaction and eventually yields azoxybenzene **5** and BEMPH$^+$-OH$^-$. Compound **5** was indeed always found to be formed in an equal amount to nitrone **3a**.

Similarly to the enolate addition step, oxidation could be mediated also by the dimer of nitrosobenzene. Within this hypothesis, the dehydrogenative step straightforwardly yields the anionic intermediate of dimeric nitrosobenzene, that is then converted to azoxybenzene **5** *via* elimination of the hydroxyl anion. The optimized TS1 geometry (Figure 5) for the reaction with $(PhNO)_2$ is lower in energy by 8.9 kcal/mol. In both TSs, The C_α-H distance is 1.53 Å and the O-H distance is 1.12 Å. The relative hydride affinity of PhNO and $(PhNO)_2$ was evaluated using two isodesmic reactions with the nitrosoaldolate, that ultimately leads to a direct comparison between nitrosobenzene monomer and dimer hydride affinity (See Scheme S1 in Supporting Information).[21,31] In both cases the isodesmic reaction favors the removal of the hydride from **Ia** and it was found that $(PhNO)_2$ was a better oxidant with respect to the monomer.
With respect to intermediate **Ia**, TS1 has an activation energy of 29.1 kcal/mol, whereas the energy related to the starting reagents is 19.5 kcal/mol, in agreement with the experimental absence of intermediates in the reaction. Similar activation energies were observed for compounds **Ih** (4-OMe), **In** (4-NO_2) and **Im** (3,4-Cl_2) (See Figure S4 in the Supporting Information).

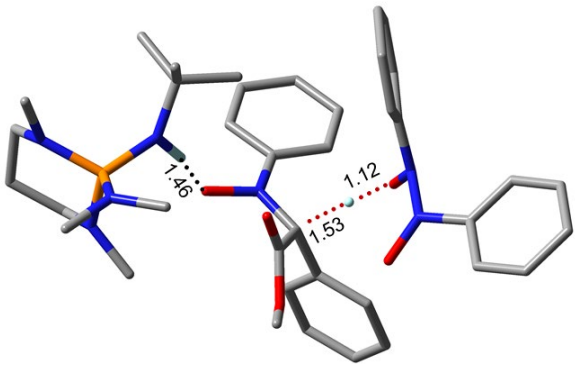

Figure 5. TS1 geometry for hydride removal from **Ia** by means of $(PhNO)_2$. Only the relevant hydrogens are shown. Distances in Å.

Pathway to imine 4

In principle, E_2 or tautomerism/$E1_{CB}$ mechanisms could be invoked for the pathway from nitrosoaldol to imine **4a**.[32] However, the intermediate nitrosoaldol bears a weak leaving group, and the carbanion is strongly stabilized into a non-protic solvent, so the $E1_{CB}$ elimination should be preferred. The *anti*-stereoselectivity of the final imines can also be explained by $E1_{CB}$ mechanism.[33] Before the $E1_{CB}$ step, the reaction pathway to imine **4a** requires the formation of nitrosoenolate **IIa**. This first step can be realized with different mechanisms. Nitrosoaldol **Ia** can be transformed into the nitrosoenolate **IIa** by the bases present in the reaction, the free BEMP, and BEMPH$^+$OH$^-$. Two TS structures were pinpointed and optimized starting from the BEMP-coordinated nitrosoaldol **I** ($TS2^1$ in and $TS2^2$ in Figure S5 of the Supporting Information).[21] Due to the steric

hindrance of BEMP, it was found that the TS where $BEMPH^+OH^-$ removes H_α from the nitrosoaldol/BEMP complex **Ia** ($TS2^1$) was much more stable than the corresponding $TS2^2$ where the free BEMP acts as the base. In $TS2^1$ the C-H_α distance is 1.37 Å and the H_α-O distance is 1.26 Å. In both geometries, the hydrogen of the nitrosoaldol is bound to the oxygen, whereas BEMP is formally neutral. Two alternative TS geometries should be therefore considered starting from the free nitrosoaldol and using $BEMPH^+OH^-$ or BEMP as the base ($TS2^3$ and $TS2^4$, Figure 6 and S5 of the Supporting Information).

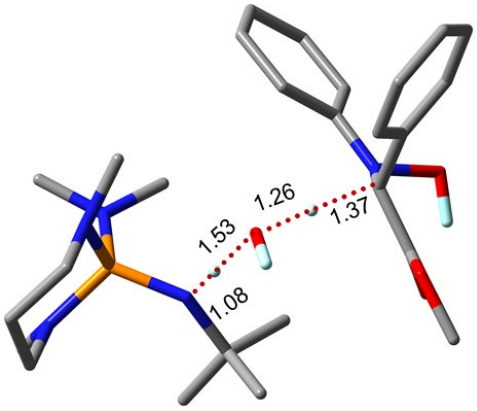

Figure 6. The best TS geometry ($TS2^3$) for tautomerism from **Ia** to nitrosoenolate **IIa**. Only the relevant hydrogens are shown. Distances in Å.

In the TS geometry, the forming enolate is stabilized by intramolecular hydrogen bond of the carbonyl with the N-OH. The C-H_α and O-H distances are 1.37 Å and 1.26Å in the TS with $BEMPH^+OH^-$ (1.61 and 1.25 Å with BEMP).[21] Among the four optimized TS2 geometries, the lowest energy corresponds to the deprotonation of the free nitrosoaldol by means of $BEMPH^+OH^-$ ($TS2^3$, Figure 6), with an activation energy of 22.4 kcal/mol (*vs* the free nitrosoaldol). However, considering the uncomplexation energy required to get the free nitrosoaldol from **Ia** (1.6 kcal/mol), the overall energy of $TS2^3$ with respect to intermediate **Ia** is 24.0 kcal/mol.

E1CB elimination

The last reaction step to imine **4** involves the $E1_{CB}$ elimination. The TS for the elimination step was optimized (Figure 7) and the calculated activation energy for compound **a** was 28.9 kcal/mol. Therefore, it turns out that the pathways to nitrone **3** and imine **4** have very similar energies. The substituents on the aryl ring of the phenylacetic ester thus play a key role in biasing the preferred pathway towards the nitrone or the imine, because of the different electronic contribution to the stabilization of the negative charge of the enolate (this contribution is also reflected on the thermodynamic acidity of H_α, see below). For this reason, the two TS geometries were optimized for three selected compounds (4-$NO_2C_6H_4$ **n**, 4-$MeOC_6H_4$ **h** and 3,4-$Cl_2C_6H_3$ **m**, see Figure S6 of the Supporting Information). Compound **m,** experimentally yielding both nitrone **3m** and imine **4m**, was selected because it can be used as a "reference standard" to normalize the other values, with the view to reducing the systematic errors in the calculations. The experimental trend is correctly reproduced by calculations. The pathway to nitrone is favored for the 4-OMe substituted reagent **1h**, whereas imine is favoured with the 4-NO_2 compound **1n**, being compound **1m** in the middle (Table S1 in the Supporting Information). Figure 8 summarizes the energies involved in the second branch of the catalytic cycle (Figure S7 of the Supporting Information shows the energetic profile of the whole catalytic cycle).

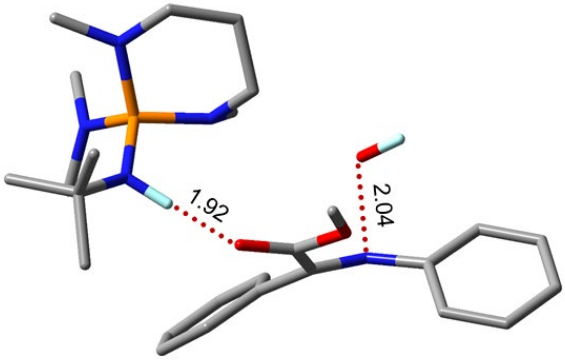

Figure 7. $E1_{CB}$ TS geometry leading to imine **4a** from nitrosoenolate **IIa**. Only the relevant hydrogens are shown. Distances in Å.

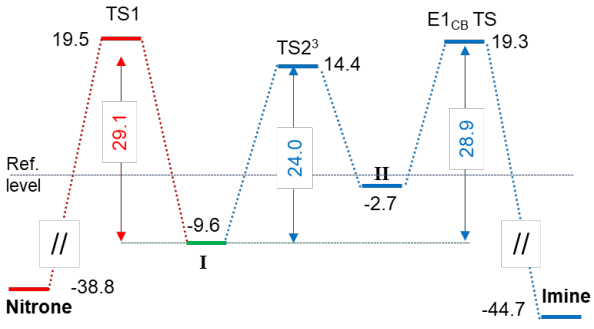

Figure 8. Second section of the catalytic cycle. The relative energies reported (in kcal/mol) are referred to the model compound **1a** at the M06-2X/6-311+G(d,p) level. The reference level is the reagents level of Figure 4.

Thermodynamic approach

Considering the previous results, it appears that the acidity of the two active hydrogens of the nitrosoaldol is a key factor for the selection of the

preferred pathway. When the N-OH is more acidic, the equilibrium with BEMP is shifted toward the ionic pair, thus H_α is less acidic and less prone to be removed by the bases present in the reaction mixture. In this case the oxidative pathway is preferred. When the NOH is less acidic, the equilibrium is more shifted toward the neutral aldol coordinated with BEMP, and the H_α is more acidic, thus stabilization of intermediate **II** and subsequent $E1_{CB}$ TS is lowered in energy.

From the thermodynamic point of view, the relative acidity of H_α with respect to N-OH can be estimated by comparison of the two isodesmic reactions, yielding the ΔpK_a between the two acidic hydrogens. (see the Supporting Information).[34] In all cases, the nitrosoaldol/BEMP complex was calculated as more stable than the nitrosoaldolate/$BEMPH^+$ ionic pair. Pleasingly, two compounds, where the calculated ΔpK_a difference is very close to zero are those where imine and nitrone are produced by the reaction in similiar amounts (**1m** and **1l**). Figure 9 shows the relationship between the calculated ΔpK_a and the experimental yield of nitrones **4**. Within this framework, our previous results, achieved in the selective α-imination of acyl pyrazoles derived from aryl acetic acid, are also rationalized.[18] In those cases, the pyrazole ring raises the acidity of the H_α to an extent where the $E1_{CB}$ pathway is always energetically preferred, likewise in the case of the 1,3-dicarbonyl compounds presented above.

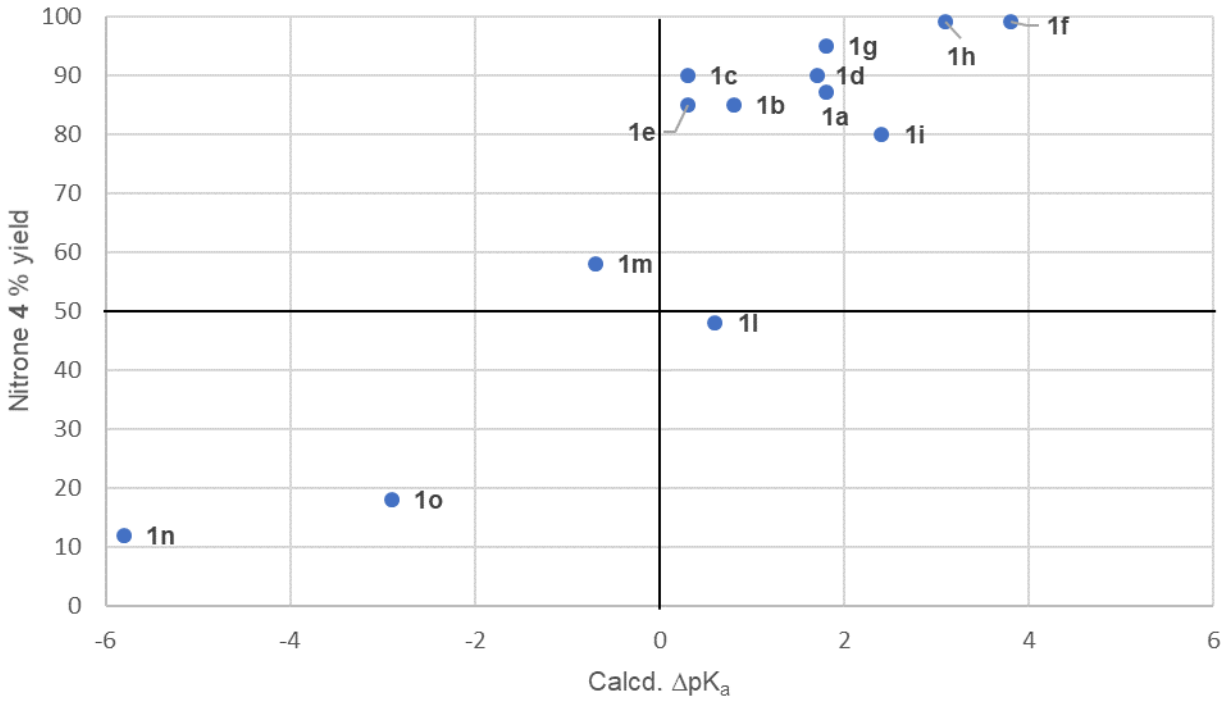

Figure 9. Relationship between calculated ΔpK_a and experimental yield of nitrones **4**. Positive values of ΔpK_a means that H_α is less acidic that N-OH.

Conclusions

We have developed a simple access to ketonitrones starting from readily available aryl acetic acid esters and nitroso arenes under catalytic basic conditions at room temperature. These compounds were rapidly obtained in good to high yield and diastereoselectivity. Synthetically, they proved to be competent reagents to obtain novel, potentially bioactive 1,2,4-oxadiazole-5-ones, via 1,3-dipolar cycloaddition. The reaction was investigated to achieve a clear mechanistic framework. A switch in the product selectivity has been observed according to the substitution pattern in the aromatic moiety of the ester. DFT calculations allowed to reproduce the whole catalytic cycle, to identify the rate-determining step (addition of enolate to PhNO). Experimental findings and DFT calculations suggested that the CH/NOH relative acidity in the firstly formed nitroso aldol intermediate **I** rules the control of the reaction pathway, and ultimately the selectivity toward nitrone or imine. The preference towards nitrone or imine was correctly reproduced by calculation of the relative acidity of N-OH and CH_α, that modifies the two competitive TS leading to nitrone or imine. This knowledge will be useful for targeted applications of the Ehrlich-Sachs type reaction to compounds suitable of enolate formation. We believe that the

present methodology will become of practical use to access ketonitrones and functionalized imines, both reagents of common use in organic synthesis.

Experimental Section

In an oven-dried vial ester **1** (0.4 mmol), nitrosoarene **2** (1.2 mmol), 3 Å molecular sieves (~90 mg) and anhydrous dichloromethane (2 mL) were introduced. To this solution BEMP (0.04 mmol) was added under nitrogen atmosphere. The reaction mixture was stirred at room temperature and monitored by TLC. After completion, the crude reaction mixture was concentrated under reduced pressure and directly purified by flash chromatography to afford products **3** and/or **4**. Computational details are reported in the Supporting Information.

Acknowledgements

This work has been supported by MIUR and University of Salerno (ORSA 168453). AM and MM thank the University of Bologna (RFO funds 2018 and 2019). Prof. I. Leito is acknowledged for useful discussions.

References

[1] a) I. A. Grigor'ev, in *Nitrile Oxides, Nitrones, and Nitronates in Organic Synthesis: Novel Strategies in Synthesis*; Second Edition, (Ed.: H. Feuer), John Wiley & Sons, Inc., Hoboken, New Jersey, **2007**; b) W. S. Jen, J. J. M. Wiener, D. W. C. MacMillan, *J. Am. Chem. Soc.* **2000**, *122*, 9874-9875; c) C. Palomo, M. Oiarbide, E. Arceo, J. M. Garcia, R. Lopez, A. Gonzalez, *Angew. Chem. Int. Ed.* **2005**, *44*, 6187-6190; *Angew. Chem.* **2005**, *117*, 6343-6346; d) P. Jiao, D. Nakashima, H. Yamamoto, *Angew. Chem. Int. Ed.* **2008**, 47, 2411-2413; *Angew. Chem.* **2008**, *120*, 2445-2447; e) M. M. Andrade, M. T. Barros, R. C. Pinto, *Tetrahedron* **2008**, *64*, 10521-10530; f) Y. Shi, A. Lin, H. Mao, Z. Mao, W. Li, H. Hu, C. Zhu, Y. Cheng, *Chem. Eur. J.* **2013**, *19*, 1914-1918; g) S.-I. Murahashi, Y. Imada, *Chem. Rev.* **2019**, *119*, 4684-4716.

[2] For selected reviews, see: a) K. V. Gothelf, K. A. Jorgensen, *Chem. Commun.* **2000**, 1449-1458; b) T. B. Nguyen, A. Martel, C. Gaulon, R. Dhal, G. Dujardin, *Org. Prep. Proced. Int.* **2010**, *42*, 387-431; c) L. L. Anderson, *Asian J. Org. Chem.* **2016**, *5*, 9-30; d) A. Brandi, F. Cardona, S. Cicchi, F. M. Cordero, A. Goti, *Org. React.* **2017**, *94*, 1-529.

[3] For selected examples, see: a) M. P. Sibi, Z. Ma, C. P. Jasperse, *J. Am. Chem. Soc.* **2005**, *127*, 5764-5765; b) X. Wang, X. Xu, P. Y. Zavalij, M. P. Doyle, *J. Am. Chem. Soc.* **2011**, 133, 16402-16405; c) X. Xu, P. J. Zavalij, M. P. Doyle, *Chem. Commun.* **2013**, *49*, 10287-10289; d) Z.-M. Zhang, P. Chen, W. Li, Y. Niu, X.-L. Zhao, J. Zhang, *Angew. Chem. Int. Ed.* **2014**, *53*, 4350-4354; *Angew. Chem.* **2014**, *126*, 4439-4443; e) S. R. Pathipati, V. Singh, L. Eriksson, N. Selander, *Org. Lett.* **2015**, *17*, 4506-4509; f) Y. Liu, J. Ao, S. Paladhi, C. E. Song, H. Yan, *J. Am. Chem. Soc.* **2016**, *138*, 16486-16492; g) C. Gelis, G. Levitre, V. Guerineau, D. Touboul, L. Neuville, G. Masson, *Eur. J. Org. Chem.* **2019**, *31*, 5151-5155.

[4] a) M. Kinugasa, S. Hashimoto, *J. Chem. Soc. Chem. Commun.* **1972**, 466-467; b) K. Okuro, M. Enna, M. Miura, M. Nomura, *J. Chem. Soc. Chem. Commun.* **1993**, 1107-1108; c) M. M.-C. Lo, G. C. Fu, *J. Am. Chem. Soc.* **2002**, *124*, 4572-4573.

[5] Bøgevig, A.; Gothelf, K. V.; Jørgensen, K. A. *Chem. Eur. J.* **2002**, *8*, 5652-5661.

[6] a) H. Chalaye-Mauger, J.-N. Denis, M.-T. Averbuch-Pouchot, Y. Vallée, *Tetrahedron* **2000**, *56*, 791-804; b) C. Berini, F. Minassian, N. Pelloux-Léon, J.-N. Denis, Y. Vallée, C. Philouze, *Org. Biomol. Chem.* **2008**, *6*, 2574-2586.

[7] I. Nakamura, D. Zhang, M. Terada, *J. Am. Chem. Soc.* **2010**, *132*, 7884-7886.

[8] a) J. Splitter, M. Calvin, *J. Org. Chem.* **1958**, *23*, 651; b) Y. Zhang, M. L. Blackman, A. B. Leduc, T. F. Jamison, *Angew. Chem. Int. Ed.* **2013**, *52*, 4251-4255; *Angew. Chem.* **2013**, *125*, 4345-4349.

[9] a) N. A. LeBel, E. G. Banucci, *J. Org. Chem.* **1971**, *36*, 2440-2448; b) P. Merino, A. Lanaspa, F. L. Merchan, T. Tejero, *Tetrahedron: Asymmetry* **1998**, *9*, 629-646; c) S. Morales, F. G. Guijarro, I. Alonso, J. L. G. Ruano, M. B. Cid, *ACS Catal.* **2016**, *6*, 84-91; d) E. Colacino, P. Nun, F. M. Colacino, J. Martinez, F. Lamaty, *Tetrahedron* **2008**, *64*, 5569-5576.

[10] For selected examples, see: a) C. Matassini, F. Cardona, *Chimia* **2017**, *71*, 558-561; b) S. Cicchi, M. Corsi, A. Goti, *J. Org. Chem.* **1999**, *64*, 7243-7245; c) C. Matassini, C. Parmeggiani, F. Cardona, A. Goti, *Org. Lett.* **2015**, *17*, 4082-4085.

[11] For selected examples, see: a) L.-D. Zhang, L.-R. Zhong, J. Xi, X.-L. Yang, Z.-J. Yao, *J. Org. Chem.* **2016**, *81*, 1899-1904; b) D.-L. Mo, D. A. Wink, L. L. Anderson, *Org. Lett.* **2012**, *14*, 5180-5183; c) I. Nakamura, T. Araki, D. Zhang, Y. Kudo, E. Kwon, M. Terada, *Org. Lett.* **2011**, *13*, 3616-3619; d) M. A. Flores, J. W. Bode, *Org. Lett.* **2010**, *12*, 1924-1927. For the use of oximes with alkenes, see: e) X. Peng, B. M. K. Tong, H. Hirao, S. Chiba, *Angew. Chem. Int. Ed*. **2014**, *53*, 1959-1962; *Angew. Chem.* **2014**, *126*, 1990-1993; f) Z. Li, J.o Zhao, B. Sun, T. Zhou, M. Liu, S. Liu, M. Zhang, Q. Zhang, *J. Am. Chem. Soc.* **2017**, 139, 11702-11705; g) M. Zhang, S. Liu, H. Li,Y. Guo, N. Li, M. Guan, H. Mehfooz, J. Zhao, Q. Zhang, *Chem. Eur. J.* **2019**, *25*, 12620-12627.

[12] For a review, see: J. Huang, Z. Chen, J. Yuan, Y. Peng, *Asian J. Org. Chem.* **2016**, *5*, 951-960.

[13] R. R. Singh, R.-S. Liu, *Chem. Commun.* **2014**, *50*, 15864-15866.

[14] A. J. Fraboni, S. E. Brenner-Moyer, *Org. Lett.* **2016**, *18*, 2146-2149.

[15] a) A. P. Chavannavar, A. G. Oliver, B. L. Ashfeld, *Chem. Commun.* **2014**, *50*, 10853-10856; b) J. Feng, P.-J. Ma, Y.-M. Zeng, Y.-J. Xu, C.-D. Lu, *Chem.*

Commun. **2018**, *54*, 2882-2885; c) A. D. Dilman, I. M. Lyapkalo, S. L. Ioffe, Y. A. Strelenko, V. A. Tartakovskii, *Zh. Org. Khim.* **1996**, *32*, 463-467.

[16] a) F. Barrow, F. J. Thorneycroft, *J. Chem. Soc.* **1934**, 722-726; b) Y.-H. Zhang, M.-Y. Wu, W.-C. Huang, *RSC Adv.* **2015**, *5*, 105825-105828.

[17] P. Ehrlich, F. Sachs, *Ber.* **1899**, *32*, 2341-2346.

[18] C. Volpe, S. Meninno, G. Mirra, A. Capobianco, A. Lattanzi, *Org. Lett.* **2019**, *21*, 5305-5309.

[19] C. Volpe, S. Meninno, A. Capobianco, G. Vigliotta, A. Lattanzi, *Adv. Synth. Catal.* **2019**, *361*, 1018-1022.

[20] M. A. Chiacchio, L. Legnani, A. Campisi, P. Bottino, G. Lanza, D. Iannazzo, L. Veltri, S. Giofrè, R. Romeo, *Org. Biomol. Chem.* **2019**, *17*, 4892-4905.

[21] a) H. Awano, T. Hirabayashi, W. Tagaki, *Tetrahedron Lett.* **1984**, *25*, 2005-2008; b) L. M. Ferreira, H. T. Chaves, A. M. Lobo, S. Prabhakar, H. S. Rzepa, *J. Chem. Soc. Chem. Commun.* **1993**, 133-134.

[22] a) A. E. Wendlandt, S. S. Stahl, *Angew. Chem. Int. Ed.* **2015**, *54*, 14638-14658; *Angew. Chem.* **2015**, *127*, 14848-14868 b) S. De Sarkar, S. Grimme, A. Studer, *J. Am. Chem. Soc.* **2010**, *132*, 1190-1191; c) M. S. Kharasch, B. S. Joshi, *J. Org. Chem.* **1957**, *22*, 1439-1443; d) X. Li, Y.Wang, Y. Wang, M. Tang, L-B Qu, Z. Li, D. Wie, *J. Org. Chem.* **2018**, *83*, 8543-8555.

[23] See Figure S1 in the Supprting Information.

[24] Gaussian 16, Revision A.03, M. J. Frisch, G. W. Trucks, H. B. Schlegel, G. E. Scuseria, M. A. Robb, J. R. Cheeseman, G. Scalmani, V. Barone, G. A. Petersson, H. Nakatsuji, X. Li, M. Caricato, A. V. Marenich, J. Bloino, B. G. Janesko, R. Gomperts, B. Mennucci, H. P. Hratchian, J. V. Ortiz, A. F. Izmaylov, J. L. Sonnenberg, D. Williams-Young, F. Ding, F. Lipparini, F. Egidi, J. Goings, B. Peng, A. Petrone, T. Henderson, D. Ranasinghe, V. G. Zakrzewski, J. Gao, N. Rega, G. Zheng, W. Liang, M. Hada, M. Ehara, K. Toyota, R. Fukuda, J. Hasegawa, M. Ishida, T. Nakajima, Y. Honda, O. Kitao, H. Nakai, T. Vreven, K. Throssell, J. A. Montgomery, Jr., J. E. Peralta, F. Ogliaro, M. J. Bearpark, J. J. Heyd, E. N. Brothers, K. N. Kudin, V. N. Staroverov, T. A. Keith, R. Kobayashi, J. Normand, K. Raghavachari, A. P. Rendell, J. C. Burant, S. S. Iyengar, J. Tomasi, M. Cossi, J. M. Millam, M. Klene, C. Adamo, R. Cammi, J. W. Ochterski, R. L. Martin, K. Morokuma, O. Farkas, J. B. Foresman, and D. J. Fox, Gaussian, Inc., Wallingford CT, 2016.

[25] I. Kaljurand, I. A. Koppel, A. Kütt, E.-I. Rõõm, T. Rodima, I. Koppel, M. Mishima, I. Leito, *J. Phys.Chem. A* **2007**, *111*, 1245-1250.

[26] The TS_e geometry shown in Figure 2 yields the Z-enolate. The second TS providing the *E*-enolate is higher in energy.

[27] a) D. Beaudoin, J. D. Wuest. *Chem. Rev.* **2016**, *116*, 258-286; b) A. J. Fraboni, A. E. Brenner-Moyer, *Org. Lett.* **2016**, *18*, 2146-2149.

[28] a) P. K. Chattaraj, U. Sarkar, D. R. Roy, *Chem. Rev.* **2006**, *106*, 2065-2091; b) R. G. Parr, L. v. Szentpály, S. Liu, *J. Am. Chem. Soc.***1999**, *121*, 1922-1924.

[29] V. S. Batista, R. H. Crabtree, S. J. Konezny, O. R. Luca, J. M. Praetorius, *New. J. Chem.* **2012**, *36*, 1141-1144.

[29] The alternative TS where H_α shifts from carbon to the nitrogen of PhNO was found to be higher in energy.

[30] X.-Q. Zhu, C.-H. Wang, *J. Phys. Chem. A* **2010**, *114*, 13244-13256.

[31] a) R. Casasnovas, M. Adrover, J. Ortega-Castro, J. Frau, J. Donoso, F. Muñoz, *J. Phys. Chem. B* **2012**, *116*, 10665-10675; b) A. K. Biswas, R. Lo, B. Ganguly, *Synlett* **2013**, *24*, 2519-2524

[32] D. E. Ortega, R. Ormazábal-Toledo, R. Contreras, R.A. Matute, *Org. Biomol. Chem.* **2019**, *17*, 9874-9882

[33] J. R. Mohrig, B. G. Beyer, A. S. Fleischhacker, A. J. Ruthenburg, S. G. John, D. A. Snyder, P. T. Nyffeler, R. J. Noll, N. D. Penner, L. A. Phillips, H. L. S. Hurley, J. S. Jacobs, C. Treitel, T. L. James, M. P. Montgomery, *J. Org. Chem.* **2012**, *77*, 2819-2828.

[34] a) K. Kaupmees, A. Trummal, I. Leito, *Croat. Chem. Acta* **2014**, 87, 385-395; b) S. Tshepelevitsh, A. Kütt, M. Lõkov, I. Kaljurand, J. Saame, A. Heering, P. G. Plieger, R. Vianello, I. Leito, *Eur. J. Org. Chem.* **2019**, 6735-6748, c) Z. B. Maksić, R. Vianello, *J. Phys. Chem. A* **2002**, *106*, 419-430.

Nitrone/Imine Selectivity Switch in Base-Catalysed Reaction of Aryl Acetic Acid Esters with Nitrosoarenes: Joint Experimental and Computational Study

Adv. Synth. Catal. **Year**, *Volume*, Page – Page

C. Volpe, S. Meninno, A. Roselli, M. Mancinelli, A. Mazzanti* and A. Lattanzi*